Electronic Supplementary Material (ESI) for Physical Chemistry Chemical Physics.

Supplementary Information

pH-dependent physicochemical properties of ornithine lipid in mono- and bilayers

Tetiana Mukhina,[†] Georg Pabst,[‡] Jean-Marie Ruysschaert,[¶] Gerald Brezesinski,[†] and Emanuel Schneck[*,†]

†*Institute for Condensed Matter Physics, TU Darmstadt, Hochschulstraße 8, 64289 Darmstadt, Germany*

‡*Insitute of Molecular Biosciences, University of Graz, Universitätsplatz 3, 8010, Graz, Austria*

¶*Laboratoire de Structure et Fonction des Membranes Biologiques, Université Libre de Bruxelles, 1050 Bruxelles, Belgium.*

E-mail: emanuel.schneck@pkm.tu-darmstadt.de

1 OL monolayer on pH 3 subphase at $T = 20°$C: GIXD patterns and tables

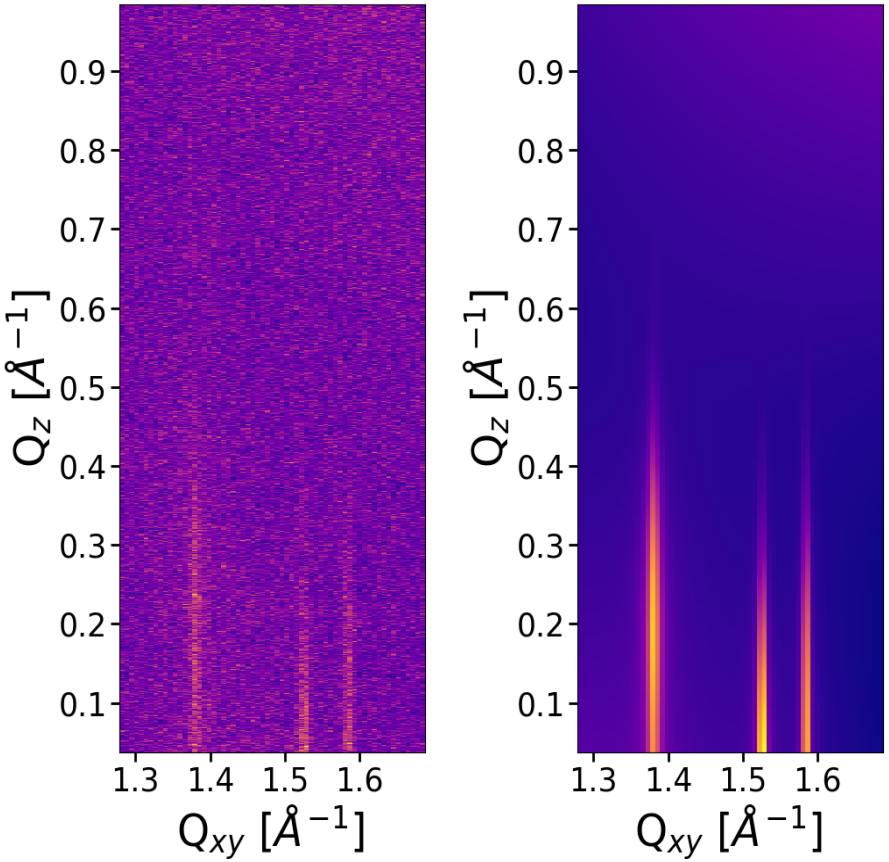

(a) (b)

Figure S1: GIXD patterns (intensity vs. in-plane component Q_{xy} and out-of-plane component Q_z of the scattering vector Q) (left) and the corresponding fits (right) of a freshly prepared OL monolayer at $\Pi = 15$ mN/m on pH 3 subphase containing additionally 1 mM $CaBr_2$.

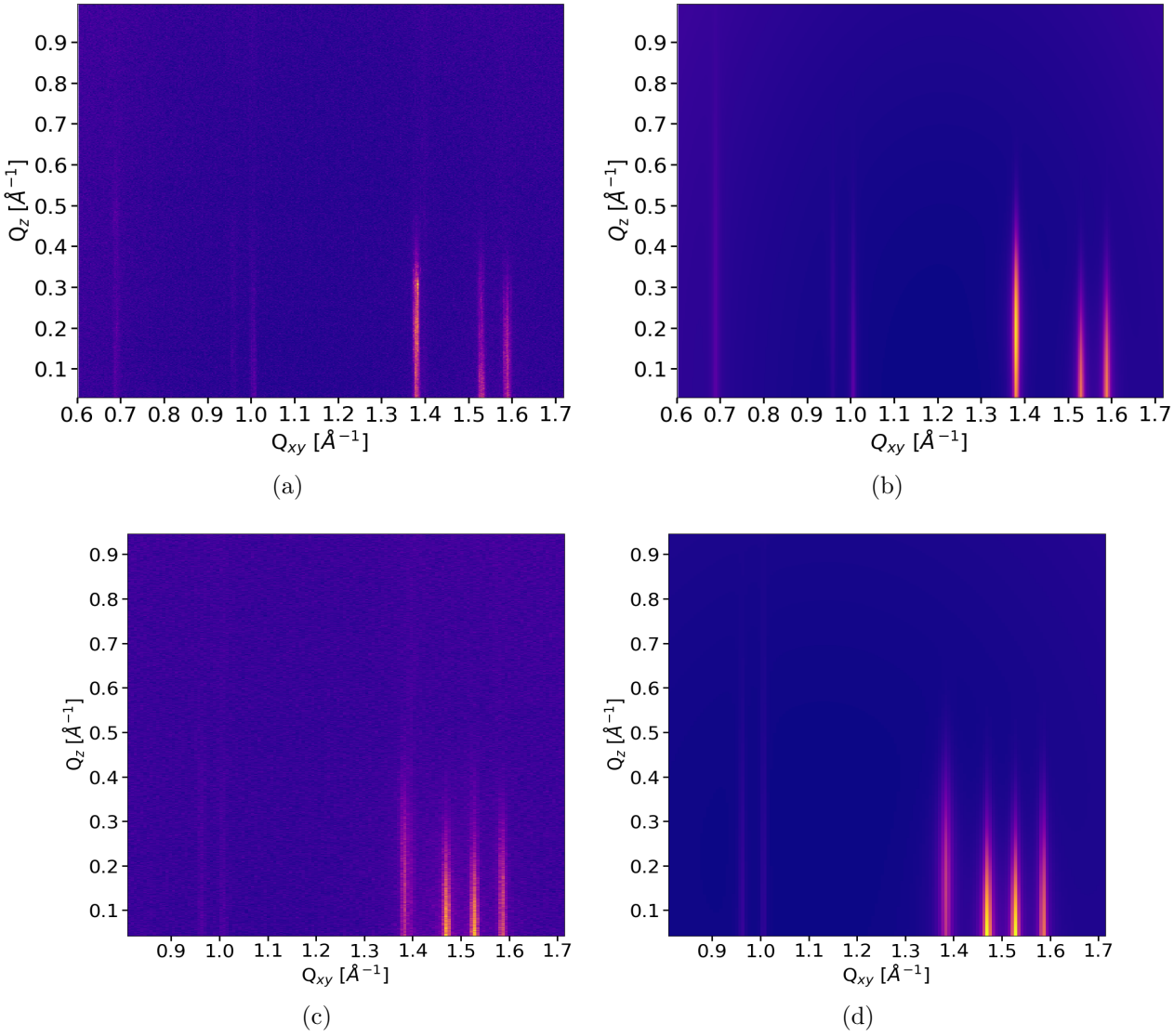

Figure S2: GIXD patterns (intensity vs. in-plane component Q_{xy} and out-of-plane component Q_z of the scattering vector Q) (left) and the corresponding fits (right) of a freshly prepared OL monolayer at $\Pi = 20$ mN/m (a, b) and at $\Pi = 30$ mN/m (c,d) on pH 3 subphase containing additionally 1 mM $CaBr_2$.

Table S1: GIXD data for a freshly prepared OL monolayer on pH 3 subphase containing additionally 1 mM $CaBr_2$. Bragg peak positions Q^0_{xy} ($\pm$ 0.003 Å^{-1}) and Q^0_z ($\pm$ 0.005 Å^{-1}) and corresponding full-widths at half-maximum FWHM(w_{xy}) ($\pm$ 0.003 Å^{-1}) and FWHM(w_z) ($\pm$ 0.005 Å^{-1}) are presented. Data in bold were used to estimate the structural parameters of the alkyl chain lattice.

Π [mN/m]	$Q^0_{xy}(1)$ [Å^{-1}]	$Q^0_z(1)$ [Å^{-1}]	$Q^0_{xy}(2)$ [Å^{-1}]	$Q^0_z(2)$ [Å^{-1}]	$Q^0_{xy}(3)$ [Å^{-1}]	$Q^0_z(3)$ [Å^{-1}]	$Q^0_{xy}(4)$ [Å^{-1}]	$Q^0_z(4)$ [Å^{-1}]	$Q^0_{xy}(5)$ [Å^{-1}]	$Q^0_z(5)$ [Å^{-1}]	$Q^0_{xy}(6)$ [Å^{-1}]	$Q^0_z(6)$ [Å^{-1}]	Data
15	**1.379**	**0.205**	**1.527**	**0.077**	**1.586**	**0.128**							Q^0
	0.014	0.346	0.006	0.346	0.005	0.346							FWHM
20	0.689	0.285	0.960	0.256	1.006	0.002	**1.381**	**0.201**	**1.531**	**0.085**	**1.590**	**0.116**	Q^0
	0.013	0.835	0.009	0.423	0.010	0.605	0.010	0.345	0.012	0.345	0.012	0.345	FWHM
30	0.959	0.100	1.004	0.101	**1.385**	**0.178**	1.471	0.047	**1.529**	**0.064**	**1.587**	**0.114**	Q^0
	0.010	0.765	0.006	0.942	0.019	0.356	0.015	0.377	0.012	0.356	0.012	0.356	FWHM

Table S2: Structural parameters obtained from GIXD data for a freshly prepared OL monolayer on pH 3 subphase containing additionally 1 mM $CaBr_2$ at $T = 20$°C. Lattice parameters a, b, c ($\pm$ 0.01 Å) and α, β, γ ($\pm$ 0.1°), lattice distortion d ($\pm$ 0.01), chain tilt t ($\pm$ 0.1°) from the surface normal, in-plane area per alkyl chain A_{xy} ($\pm$ 0.1 Å^2) and chain cross-sectional area A_0 ($\pm$ 0.1 Å^2).

Π [mN/m]	a, b, c [Å]	α, β, γ [°]	d	t [°]	A_{xy} [Å^2]	A_0 [Å^2]
15	4.51	127.5	0.16	8.5	20.5	20.3
	4.99	118.5				
	5.18	114.1				
20	4.49	127.5	0.16	8.3	20.5	20.2
	4.98	118.5				
	5.17	114.1				
30	4.51	127.3	0.16	7.4	20.4	20.3
	4.97	118.5				
	5.16	114.2				

1.1 Molecular supperlatice of a freshly prepared OL monolayer on pH 3 subphase

The chain lattice of a freshly prepared OL monolayer (Tab. S2) on pH 3 subphase at $\Pi = 20$ mN/m at $T = 20$°C is defined by the following lattice parameters: $a = 4.49$ Å, $b = 4.98$ Å, and $\gamma = 114.1$ °. The chains are slightly tilted (tilt angle $\simeq 8$°) and packed with a cross-sectional area of $A_0 = 20.2$ Å^2, which is typical for phospholipids in the gel state. Based on this chain lattice, a molecular superlattice with $a_s = 13.47$ Å, $b_s = 9.96$ Å, $\gamma = 114.1$ ° was estimated following the procedure described elsewhere.[1–3] The in-plane area is $A_{xy} = 122.5$ Å^2 of the defined molecular lattice is commensurate with three OL molecules (corresponding to the six chains with $A_{xy} = 20.4$ Å^2).

Table S3: Experimental and calculated GIXD peak positions and Miller indexes of the molecular super lattice for a freshly prepared OL monolayer on pH 3 subphase containing additionally 1 mM $CaBr_2$ at $T = 20$°C.

Q^0_{xy}(exp) [Å^{-1}]	Q^0_{xy}(cal) [Å^{-1}]	(h, k)
0.689	0.691	(0 1), (0 -1)
0.960	0.972	(-2 1), (2 -1)
1.006	1.013	(-1 -1), (1 1)
1.381	1.382	(0 -2), (0 2)
1.531	1.533	(-3 0), (3 0)
1.590	1.591	(3 -2), (-3 2)

2 OL monolayer on pH 10 subphase at $T = 20°C$. GIXD patterns and tables

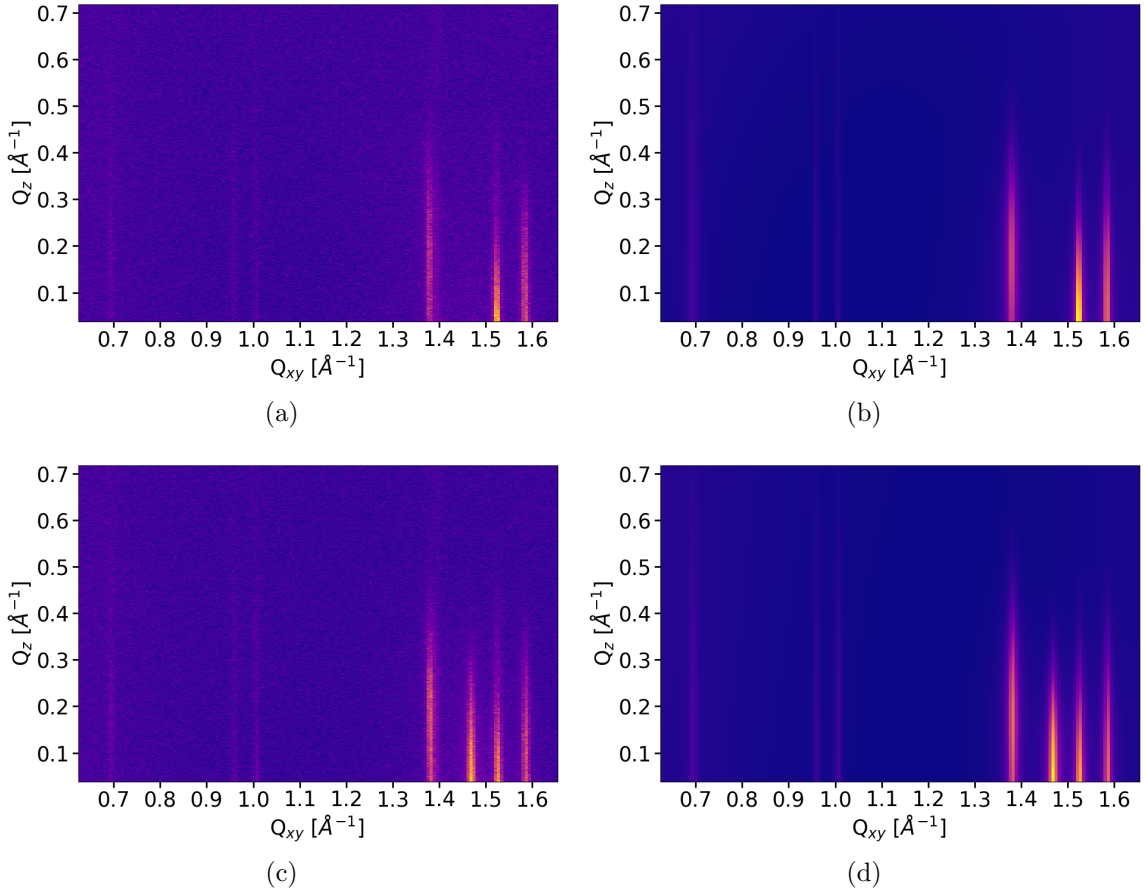

Figure S3: GIXD patterns (intensity vs. in-plane component Q_{xy} and out-of-plane component Q_z of the scattering vector Q) (a, c) and the corresponding fits (b, d) of a freshly prepared OL monolayer at $\Pi = 21$ mN/m (a, b) and at $\Pi = 30$ mN/m (c, d) on pH 10 subphase containing additionally 1 mM $CaBr_2$.

Table S4: GIXD data for a freshly prepared OL monolayer on pH 10 subphase containing additionally 1 mM $CaBr_2$. Bragg peak positions Q^0_{xy} ($\pm$ 0.003 Å^{-1}) and Q^0_z ($\pm$ 0.005 Å^{-1}) and corresponding full-widths at half-maximum FWHM(w_{xy}) ($\pm$ 0.003 Å^{-1}) and FWHM(w_z) ($\pm$ 0.005 Å^{-1}) are presented. Data in bold were used to estimate the structural parameters of the alkyl chain lattice.

Π [mN/m]	$Q^0_{xy}(1)$ [Å^{-1}]	$Q^0_z(1)$ [Å^{-1}]	$Q^0_{xy}(2)$ [Å^{-1}]	$Q^0_z(2)$ [Å^{-1}]	$Q^0_{xy}(3)$ [Å^{-1}]	$Q^0_z(3)$ [Å^{-1}]	$Q^0_{xy}(4)$ [Å^{-1}]	$Q^0_z(4)$ [Å^{-1}]	$Q^0_{xy}(5)$ [Å^{-1}]	$Q^0_z(5)$ [Å^{-1}]	$Q^0_{xy}(6)$ [Å^{-1}]	$Q^0_z(6)$ [Å^{-1}]	$Q^0_{xy}(7)$ [Å^{-1}]	$Q^0_z(7)$ [Å^{-1}]	Data
21	0.690	0.100	0.958	0.169	1.004	0.035	**1.381**	**0.182**	**1.526**	**0.056**	**1.586**	**0.126**			Q^0
	0.020	0.838	0.001	0.566	0.001	0.768	0.017	0.322	0.008	0.322	0.009	0.322			FWHM
30	0.691	0.038	0.958	0.035	1.005	0.009	**1.383**	**0.184**	1.471	0.063	**1.528**	**0.067**	**1.588**	**0.117**	Q^0
	0.013	0.853	0.005	0.759	0.007	0.754	0.016	0.338	0.015	0.353	0.012	0.338	0.012	0.338	FWHM

Table S5: Structural parameters obtained from GIXD data for a freshly prepared OL monolayer on pH 10 subphase containing additionally 1 mM $CaBr_2$. Lattice parameters a, b, c ($\pm$ 0.01 Å) and α, β, γ ($\pm$ 0.1°), lattice distortion d ($\pm$ 0.01), chain tilt t ($\pm$ 0.1°) from the surface normal, in-plane area per alkyl chain A_{xy} ($\pm$ 0.1 Å^2) and chain cross-sectional area A_0 ($\pm$ 0.1 Å^2).

Π [mN/m]	a, b, c [Å]	α, β, γ [°]	d	t [°]	A_{xy} [Å^2]	A_0 [Å^2]
21	4.51	127.4	0.16	7.6	20.5	20.3
	4.98	118.6				
	5.18	114.0				
30	4.50	127.4	0.16	7.6	20.5	20.3
	4.98	118.6				
	5.17	114.0				

3 OL monolayer on pH 6 subphase at $T = 20°C$. GIXD patterns and tables

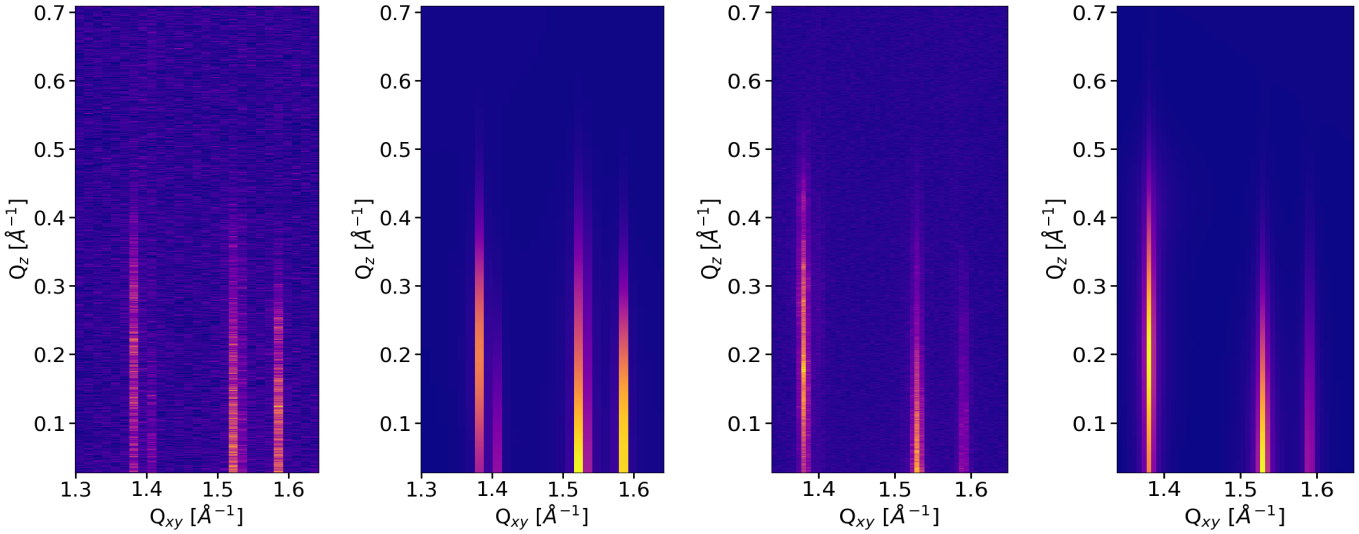

(a) (b) (c) (d)

Figure S4: GIXD patterns (intensity vs. in-plane component Q_{xy} and out-of-plane component Q_z of the scattering vector Q) (a, c) and the corresponding fits (b, d) of a freshly prepared OL monolayer at $\Pi = 10$ mN/m (a, b) and at $\Pi = 15$ mN/m (c, d) on pH 6 subphase containing additionally 1 mM $CaBr_2$.

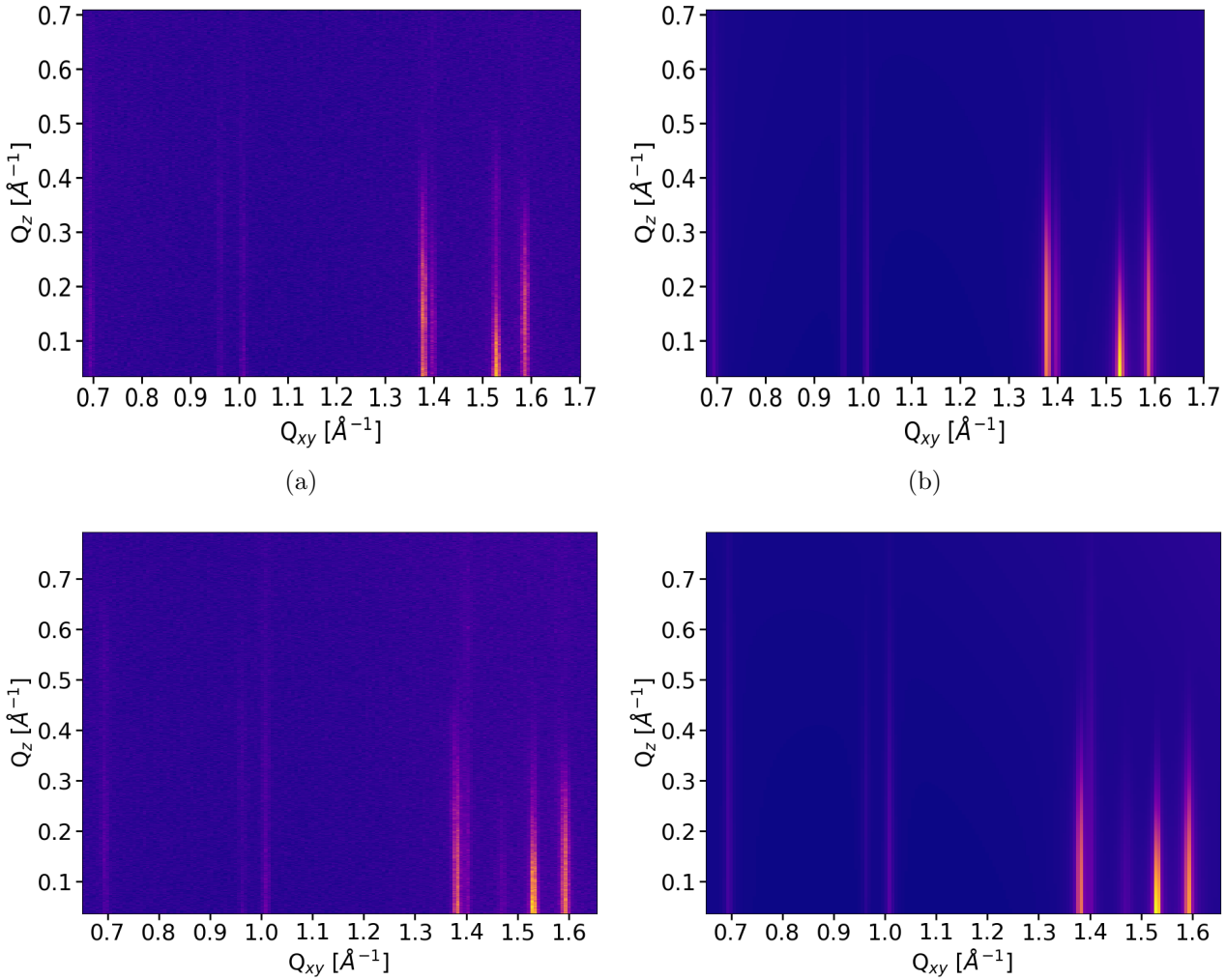

Figure S5: GIXD patterns (intensity vs. in-plane component Q_{xy} and out-of-plane component Q_z of the scattering vector Q) (a, c) and the corresponding fits (b, d) of a freshly prepared OL monolayer at $\Pi = 20$ mN/m (a, b) and at $\Pi = 30$ mN/m (c, d) on pH 6 subphase containing additionally 1 mM $CaBr_2$.

Table S6: GIXD data for a freshly prepared OL monolayer on pH 6 subphase containing additionally 1 mM $CaBr_2$. Bragg peak positions Q^0_{xy} ($\pm$ 0.003 Å^{-1}) and Q^0_z ($\pm$ 0.005 Å^{-1}) and corresponding full-widths at half-maximum FWHM(w_{xy}) ($\pm$ 0.003 Å^{-1}) and FWHM(w_z) ($\pm$ 0.005 Å^{-1}) are presented. Data in bold were used to estimate the structural parameters of the alkyl chain lattice.

Π [mN/m]	$Q^0_{xy}(1)$ [Å^{-1}]	$Q^0_z(1)$ [Å^{-1}]	$Q^0_{xy}(2)$ [Å^{-1}]	$Q^0_z(2)$ [Å^{-1}]	$Q^0_{xy}(3)$ [Å^{-1}]	$Q^0_z(3)$ [Å^{-1}]	$Q^0_{xy}(4)$ [Å^{-1}]	$Q^0_z(4)$ [Å^{-1}]	$Q^0_{xy}(5)$ [Å^{-1}]	$Q^0_z(5)$ [Å^{-1}]	$Q^0_{xy}(6)$ [Å^{-1}]	$Q^0_z(6)$ [Å^{-1}]	$Q^0_{xy}(7)$ [Å^{-1}]	$Q^0_z(7)$ [Å^{-1}]	$Q^0_{xy}(8)$ [Å^{-1}]	$Q^0_z(8)$ [Å^{-1}]	Data
10	**1.379**	**0.208**	1.401	0.045	**1.528**	**0.119**	1.523	0.034	**1.586**	**0.089**							Q^0
	0.008	0.350	0.001	0.306	0.001	0.350	0.001	0.103	0.003	0.350							FWHM
15	**1.379**	**0.203**	1.385	0.427	**1.530**	**0.092**	**1.592**	**0.111**									Q^0
	0.010	0.332	0.043	0.142	0.011	0.332	0.007	0.332									FWHM
20	0.690	0.018	0.958	0.223	1.005	0.006	**1.380**	**0.156**	1.401	0.143	**1.531**	**0.010**	**1.589**	**0.146**			Q^0
	0.013	0.910	0.003	0.466	0.006	0.661	0.008	0.324	0.000	0.311	0.011	0.324	0.012	0.324			FWHM
30	0.692	0.152	0.962	0.243	1.008	0.005	**1.382**	**0.136**	1.402	0.183	1.472	0.007	**1.533**	**0.016**	**1.594**	**0.120**	Q^0
	0.010	0.924	0.011	0.499	0.011	0.779	0.009	0.342	0.014	0.706	0.023	0.445	0.008	0.342	0.012	0.342	FWHM

Table S7: Structural parameters obtained from GIXD data for a freshly prepared OL monolayer on pH 6 subphase containing additionally 1 mM $CaBr_2$. Lattice parameters a, b, c ($\pm$ 0.01 Å) and α, β, γ ($\pm$ 0.1°), lattice distortion d ($\pm$ 0.01), chain tilt t ($\pm$ 0.1°) from the surface normal, in-plane area per alkyl chain A_{xy} ($\pm$ 0.1 Å^2) and chain cross-sectional area A_0 ($\pm$ 0.1 Å^2).

Π [mN/m]	a, b, c [Å]	α, β, γ [°]	d	t [°]	A_{xy} [Å^2]	A_0 [Å^2]
10	4.50 4.99 5.18	127.5 118.5 114.0	0.16	8.6	20.5	20.3
15	4.49 4.98 5.18	127.6 118.5 113.9	0.16	8.4	20.5	20.3
20	4.50 4.98 5.17	127.5 118.4 114.1	0.16	6.9	20.5	20.3
30	4.48 4.97 5.17	127.6 118.5 113.9	0.16	5.9	20.4	20.3

4 Cyclic OL

When storing OL in $CHCl_3$ solutions for extended periods of time, different isotherms are obtained, depending on the storage time (Fig. S6 B). For OL solutions that have aged for more than two weeks, identical isotherms (Fig. S6 C) are observed on subphases with pH 10 (blue) and pH 3 (red). The LE/LC transition occurs at $\Pi \approx 21$ mN/m. The transition is very sharp and the plateau region is rather flat with no surface-inhibited nucleation. The isotherm of OL stored for 5 days combines the features of both the freshly prepared OL solution and the aged solution, suggesting coexistence of OL with stretched and cyclic headgroups. Fig. S6 D illustrates the chemical structure of cyclic OL. The first transition occurs on compression at higher lateral pressures compared to the freshly prepared OL solution, which may reflect partial mixing of the compounds with linear and cyclic headgroups. GIXD experiments on monolayers of aged OL solutions at low and high pH reveal only one Bragg peak at at $Q_{xy} = 1.47$ Å^{-1} (Fig. S6 A), which is characteristic for a hexagonal packing of non-tilted chains without any molecular superlattice. With 21 Å^2, the determined chain-cross-sectional area is surprisingly large. TRXF was again used to determine the presence of charges in the monolayer by counting the counterions Br^- and Ca^{2+}. At both pH values investigated (3 and 10), only a marginal attraction of ions to the monolayer of OL with a cyclic headgroup is observed, indicating that aged OL monolayers are practically non-charged. Closer inspection of the GIXD data of monolayers even from freshly prepared OL solutions reveals the appearance of an additional Bragg peak at $Q_{xy} = 1.47$ Å^{-1} at high lateral pressure (30 mN/m, see Fig. S2 C). This peak coincides with the single peak observed for monolayers of aged and thus cyclic OL, indicating that traces of cyclic OL are present in the monolayer under these conditions, in the form of a segregated phase coexisting with the majority SL phase of the regular OL molecules. The following two scenarios are imaginable: Either there are already traces of cyclic OL present in the freshly prepared solutions, and the peak then only emerges at sufficiently high lateral pressure above the phase transition of the cyclic compound at $\Pi \approx 21$ mN/m (Fig. S6 C). Or compression leads to an advantageous

headgroup orientation triggering cyclization. At the moment, we cannot exclude either of the two possibilities.

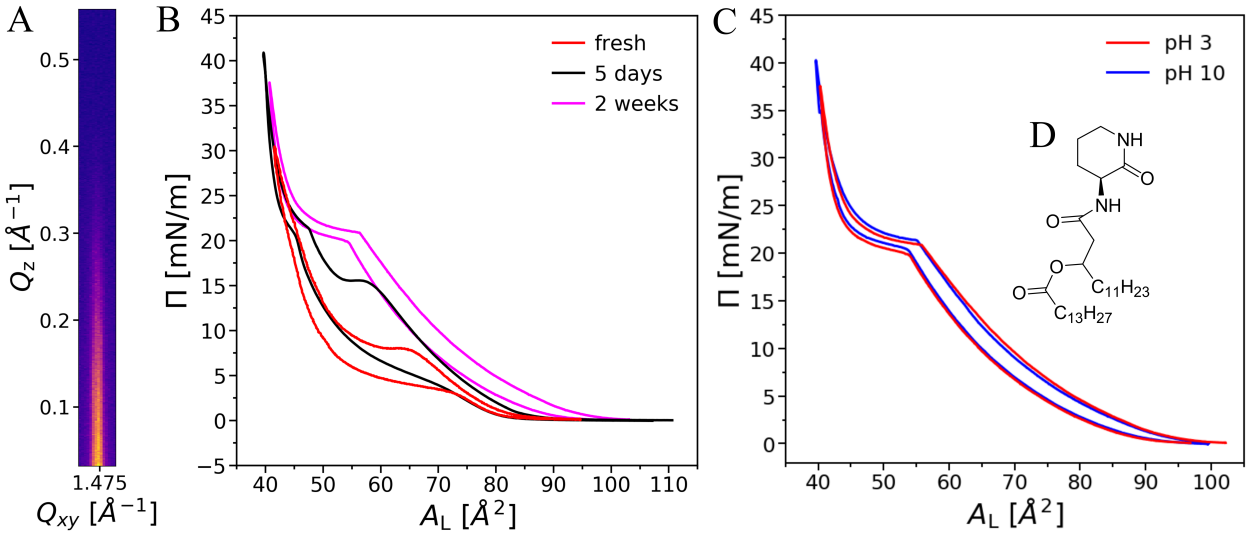

Figure S6: (A) GIXD data (Intensity vs in-plane component Q_{xy} and the out-of-plane component Q_z of the scattering vector Q) for a monolayer spread from an aged (2-weeks-old) OL solution at $\Pi = 30$ mN/m on pH 3 subphase containing additionally 1 mM $CaBr_2$ at $T = 20$°C . (B) Monolayer isotherms of OL in $CHCl_3$ solution (freshly prepared (red), stored for 5 days (black), and stored for at least 2 weeks (magenta) on pH 3 (red and magenta) or water (black) subphases containing additionally 1 mM $CaBr_2$. (C) Monolayer isotherms of OL stored in $CHCl_3$ solution for at least 2 weeks on pH 10 (blue) and pH 3 (red) subphases at $T = 20$°C. (D) Chemical structure of cyclic OL.

4.1 Monolayer from an aged OL solution on pH 2.8 subphase at $T = 20°C$. GIXD patterns and tables

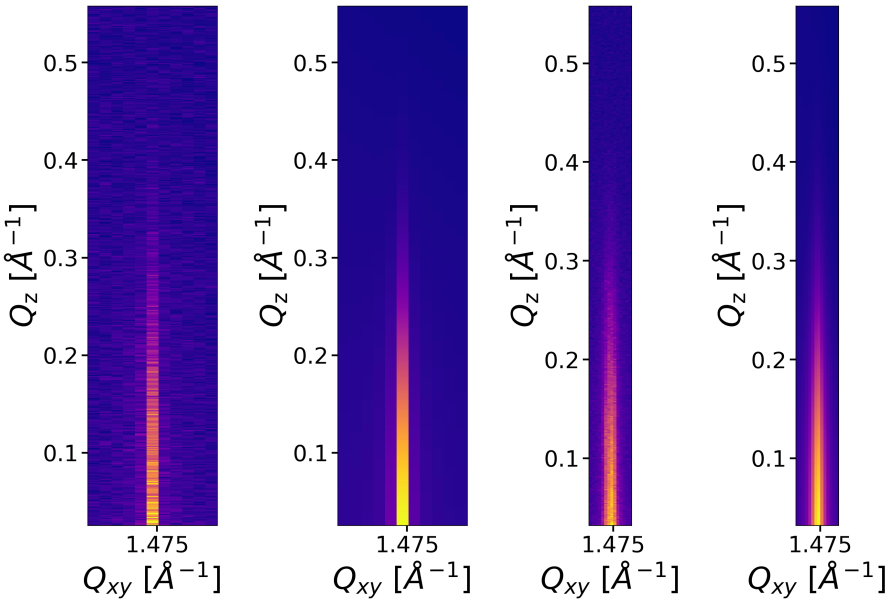

Figure S7: GIXD patterns (intensity vs. in-plane component Q_{xy} and out-of-plane component Q_z of the scattering vector Q) (a, c) and the corresponding fits (b, d) for a monolayer from an aged (2-weeks-old) OL solution at $\Pi = 24$ mN/m (a, b) and at $\Pi = 30$ mN/m (c, d) on pH 2.8 subphase containing additionally 1 mM $CaBr_2$.

Table S8: GIXD data for a monolayer from an aged (2-weeks-old) OL solution on pH 2.8 subphase containing additionally 1 mM $CaBr_2$. Bragg peak positions Q^0_{xy} ($\pm$ 0.003 Å^{-1}) and Q^0_z ($\pm$ 0.005 Å^{-1}) and corresponding full-widths at half-maximum FWHM(w_{xy}) ($\pm$ 0.003 Å^{-1}) and FWHM(w_z) ($\pm$ 0.005 Å^{-1}) are presented.

Π [mN/m]	$Q^0_{xy}(1)$ [Å^{-1}]	$Q^0_z(1)$ [Å^{-1}]	Data
24	1.469	0.000	Q^0
	0.010	0.353	FWHM
30	1.473	0.000	Q^0
	0.012	0.353	FWHM

Table S9: Structural parameters obtained from GIXD data for a monolayer from an aged (2-weeks-old) OL solution on pH 2.8 subphase containing additionally 1 mM $CaBr_2$. Lattice parameters a, b, c ($\pm$ 0.01 Å) and α, β, γ ($\pm$ 0.1°), lattice distortion d ($\pm$ 0.01), chain tilt t ($\pm$ 0.1°) from the surface normal, in-plane area per alkyl chain A_{xy} ($\pm$ 0.1 Å^2) and chain cross-sectional area A_0 ($\pm$ 0.1 Å^2).

Π [mN/m]	a, b, c [Å]	α, β, γ [°]	d	t [°]	A_{xy} [Å^2]	A_0 [Å^2]
24	4.94	120.0	0	0	21.1	21.1
	4.94	120.0				
	4.94	120.0				
30	4.93	120.0	0	0	21.0	21.0
	4.93	120.0				
	4.93	120.0				

4.2 Aged OL monolayer on pH 10.1 subphase at $T = 20$°C. GIXD patterns and tables

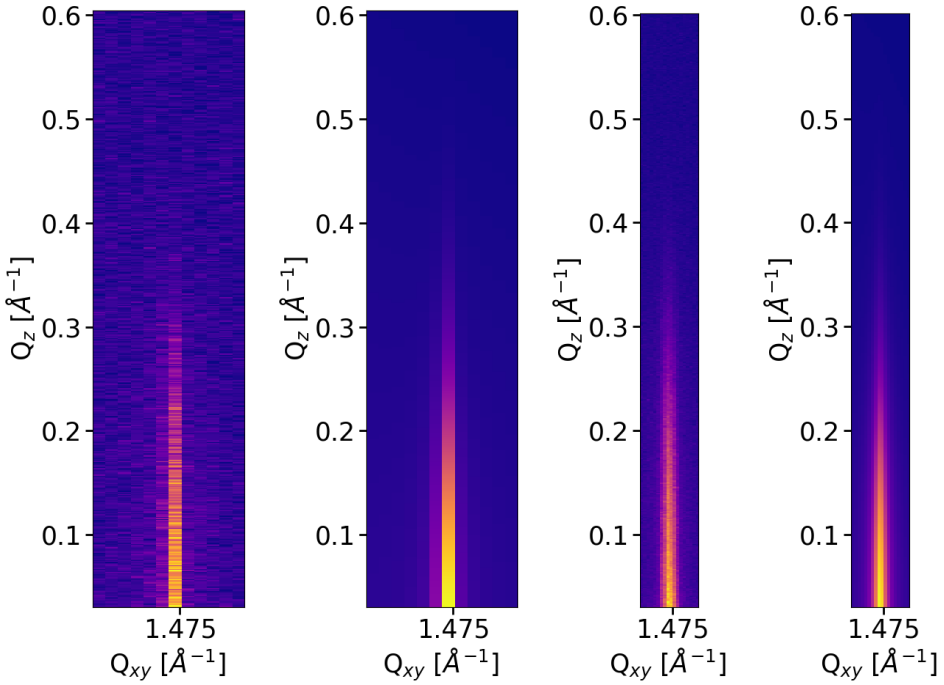

Figure S8: GIXD patterns (intensity vs. in-plane component Q_{xy} and out-of-plane component Q_z of the scattering vector Q) (a, c) and the corresponding fits (b, d) for a monolayer from an aged (2-weeks-old) OL solution at $\Pi = 24$ mN/m (a, b) and at $\Pi = 30$ mN/m (c, d) on pH 10.1 subphase containing additionally 1 mM $CaBr_2$.

Table S10: GIXD data for a monolayer from an aged (2-weeks-old) OL solution on pH 10.1 subphase containing additionally 1 mM $CaBr_2$. Bragg peak positions Q^0_{xy} ($\pm$ 0.003 Å^{-1}) and Q^0_z ($\pm$ 0.005 Å^{-1}) and corresponding full-widths at half-maximum FWHM(w_{xy}) ($\pm$ 0.003 Å^{-1}) and FWHM(w_z) ($\pm$ 0.005 Å^{-1}) are presented.

Π [mN/m]	$Q^0_{xy}(1)$ [Å^{-1}]	$Q^0_z(1)$ [Å^{-1}]	Data
24	1.468	0.000	Q^0
	0.010	0.353	FWHM
30	1.472	0.000	Q^0
	0.012	0.353	FWHM

Table S11: Structural parameters obtained from GIXD data for a monolayer from an aged (2-weeks-old) OL solution on pH 10.1 subphase containing additionally 1 mM $CaBr_2$. Lattice parameters a, b, c ($\pm$ 0.01 Å) and α, β, γ ($\pm$ 0.1°), lattice distortion d ($\pm$ 0.01), chain tilt t ($\pm$ 0.1°) from the surface normal, in-plane area per alkyl chain A_{xy} ($\pm$ 0.1 Å^2) and chain cross-sectional area A_0 ($\pm$ 0.1 Å^2).

Π [mN/m]	a, b, c [Å]	α, β, γ [°]	d	t [°]	A_{xy} [Å^2]	A_0 [Å^2]
24	4.94	120	0	0	21.2	21.2
	4.94	120				
	4.94	120				
30	4.93	120	0	0	21.0	21.0
	4.93	120				
	4.93	120				

References

(1) Stefaniu, C.; Latza, V. M.; Gutowski, O.; Fontaine, P.; Brezesinski, G.; Schneck, E. Headgroup-Ordered Monolayers of Uncharged Glycolipids Exhibit Selective Interactions with Ions. *The Journal of Physical Chemistry Letters* **2019**, *10*, 1684–1690.

(2) Stefaniu, C.; Vilotijevic, I.; Santer, M.; Varón Silva, D.; Brezesinski, G.; Seeberger, P. H. Subgel Phase Structure in Monolayers of Glycosylphosphatidylinositol Glycolipids. *Angewandte Chemie International Edition* **2012**, *51*, 12874–12878.

(3) Mukhina, T.; Brezesinski, G.; Shen, C.; Schneck, E. Phase behavior and miscibility in

lipid monolayers containing glycolipids. *Journal of Colloid and Interface Science* **2022**, *615*, 786–796.